32 phase×32 amplitude optical arbitrary waveform generation

N. K. Fontaine, R. P. Scott, J. Cao, A. Karalar, W. Jiang, K. Okamoto, J. P. Heritage, B. H. Kolner, and S. J. B. Yoo

Department of Electrical and Computer Engineering, University of California, Davis, Davis, California 95616, USA

Received October 4, 2006; accepted December 14, 2006;
posted January 18, 2007 (Doc. ID 75699); published March 5, 2007

We describe the precise shaping and mode-resolved amplitude and phase characterization of optical arbitrary waveforms by using a 20 GHz optical frequency comb and integrated 64×20 GHz channel arrayed waveguide grating pair. Complex waveforms with large variations in phase and amplitude between adjacent modes were generated and characterized. © 2007 Optical Society of America

OCIS codes: 320.7100, 320.5540.

The generation of an arbitrary waveform has many possible applications in optical communications, spectroscopy, and RF waveform generation.[1,2] In principle, direct access to the amplitude and phase of the optical spectrum makes optical arbitrary waveform generation (OAWG) feasible at bandwidths comparable with optical carrier frequencies. Usually waveform generation is accomplished by manipulating the spectral phase and spectral amplitude of an optical pulse rather than directly in the time domain. Bulk-optic pulse shapers can provide access to the optical spectrum with high resolution but lack the portability and stability required for many applications.[3] In this Letter, we use a fully integrated silica-based arrayed waveguide grating (AWG) pair pulse shaper (AWGPS) that has sufficient resolution to accurately manipulate the phase and amplitude of individual modes of a 20 GHz optical comb produced by an optical frequency comb generator (OFCG) similar to the OFCG in Ref. 4. Characterization of the mode-by-mode phase and amplitude is accomplished with cross-correlation frequency-resolved optical gating (XFROG).

Three components are necessary and crucial for OAWG. A stable set of spectral modes must be produced, a device to independently manipulate the amplitude and phase of each mode must be employed, and precise characterization of the amplitude and phase of each mode must be made. The experimental setup shown in Fig. 1 contains a stable OFCG followed by an AWGPS that independently controls the phase and amplitude of each mode. A 10 GHz harmonically mode-locked fiber laser producing 3 ps optical pulses provides the reference pulse for precise XFROG characterization of the waveform. It is synchronized to the OFCG by dividing the 20 GHz microwave signal in half by using a clock divider.

The OFCG is stable, center-wavelength and comb-spacing tunable and produces a large number of modes that are nearly uniform in amplitude with fixed phases. Strong phase modulation (PM) of an optical carrier generates spectral modes linearly proportional to the peak phase deviation spaced at the modulation frequency. Pure PM produces modes following a Bessel function expansion. The comb is flattened by applying additional amplitude modulation (AM) and is shown in Figs. 2(a) and 2(c). The OFCG consists of a tunable single-frequency laser input into a $LiNbO_3$ dual-electrode Mach–Zehnder modulator (Fig. 1, DEMZM) followed by a low V_π $LiNbO_3$ phase modulator. The phase modulator is driven with +33 dBm of RF power (signal RF3) to create 30 comb lines, while signals RF1 and RF2 drive the DEMZM. The amount of PM and AM occurring in the DEMZM depends on the relative phase and amplitude between signals RF1 and RF2 and the modulator DC bias.[4] The phase of signal RF3 is adjusted to maximize the number of modes. The output signal is split and sent to an optical spectrum analyzer (OSA) and the XFROG.

In general, the FROG technique measures the spectrogram created from two pulses.[5] An iterative algorithm retrieves the electric fields that construct the same spectrogram. In particular, XFROG allows for characterization of weak waveforms without the common ambiguities such as direction of time from which cross-correlation, autocorrelation, and second-harmonic generation FROG (SHG-FROG) measurements suffer. In addition to complete characterization, XFROG traces provide an intuitive picture of an optical pulse.

To characterize each mode of a waveform, the XFROG algorithm must be modified to account for the periodicity of the pulse train, and careful considerations in processing the measured data must be used.[6,7] The measured spectogram is prepared for the XFROG algorithm by sampling it onto a discrete 2D grid of evenly spaced frequencies and times (i.e.,

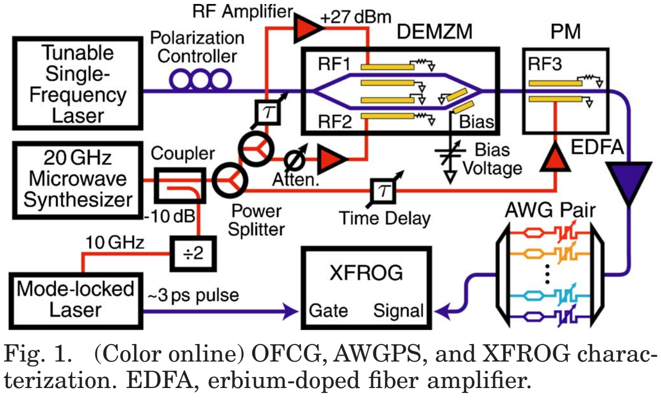

Fig. 1. (Color online) OFCG, AWGPS, and XFROG characterization. EDFA, erbium-doped fiber amplifier.

 © 2007 Optical Society of America

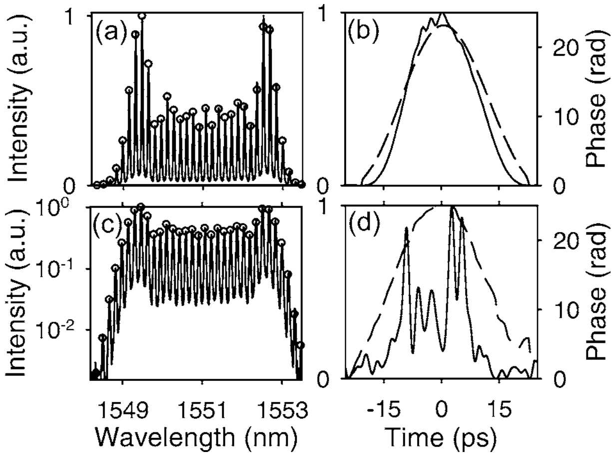

Fig. 2. Directly measured spectrum of OFCG output (lines) compared with XFROG retrieved spectrum (circles) on (a) linear and (c) logarithmic scales. (b) Intensity (solid) and phase (dashed) of time domain waveforms of OFCG output. (d) Distortion of waveform after accumulating phase errors in AWGPS.

bins). The bin spacings in the frequency and time domains are linked to one another by a Fourier transform. The time window is equal to the inverse of the bin spacing. If more information is needed in either domain, the number of sampling points is increased. The FROG algorithm characterizes only the frequencies and time points sampled in each bin. For mode-by-mode characterization, the bin spacing must be a submultiple of the mode spacing, ensuring that any bin contains exactly one mode. This prevents undersampling of the retrieved spectrum and spreading of the modes across two adjacent frequency bins. The spectral binning requirement constrains the time window to be a multiple of the waveform repetition period. Under these considerations, all time and frequency information of the waveform are stored in the XFROG trace. In this Letter, the frequency bin spacing is 20 GHz, corresponding to the time window of 50 ps. Although only 64 frequency bins are needed to sample each mode, 128 time and frequency bins are used to provide immunity to noise.[5]

The XFROG spectrometer need not resolve individual modes. The resolution only needs to be greater than the finest spectral feature in the XFROG trace. The multiplication of the signal by the gate pulse filters temporal details outside the gate pulse, broadening spectral information. Each spectral component in the XFROG trace is convolved with the frequency filter function with the same spectral width as the gate pulse. This suggests that spectrometer resolution does not need to resolve individual modes. However, resolving individual modes should facilitate increased accuracy of aligning modes to their proper bins. As an example, Figs. 3(a) and 3(b) depict an SHG-FROG trace of the waveform in Fig. 5(e). The SHG-FROG trace has complex mode-by-mode variation. However, the XFROG trace of the same pulse has slower varying spectral features. A critical and necessary requirement for binning is that the frequency sampled in each bin must be the same frequency as the modes. Otherwise, the retrieved spectra are distorted. SHG-FROG retrieved gate pulses had a FROG error, G, better (less) than $G=0.0008$, and all XFROG data had better (less) than $G=0.0038$.

To demonstrate XFROG mode-by-mode characterization, the output of the OFCG is measured with an OSA and compared with the retrieved XFROG spectrum (Fig. 2). The retrieved and independently measured spectra match well on both a log scale and a linear scale. In addition, the retrieved time domain waveform shows the applied sinusoidal amplitude and PM from the DEMZM.

The AWGPS consist of two AWGs with 64×20 GHZ wavelength channels. The input AWG spectrally demultiplexes the input signal to the wavelength channels. The second AWG multiplexes all wavelengths to the output. The temperature of each AWG is controlled to maximize the AWG's spectral overlap by maximizing the power of the optical comb through the device. Each wavelength channel provides AM and PM via a resistive-heater-based Mach–Zehnder modulator and phase modulator, respectively. The Mach–Zehnder modulator shows moderate polarization dependence (2 dB variations between the two principle polarizations), whereas the phase modulators exhibit negligible polarization dependence. Polarization control on the input to the AWGPS is adjusted to achieve maximum AM or minimal throughput. Figure 4(a) shows two channels of the transfer function of the AWG pair by measuring the phase of the AM on a single-frequency laser at different wavelengths. The OFCG is aligned to the peak of the passbands, where differential variation in phase and amplitude are minimal.

When two adjacent comb lines are incident upon a photodetector, the phase of the electrical beat signal

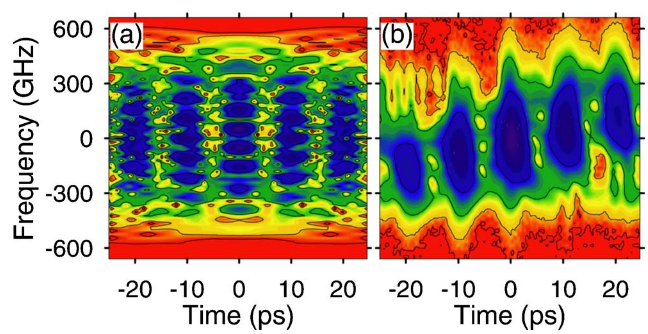

Fig. 3. (Color online) (a) Generated SHG-FROG trace and (b) measured XFROG trace of pulse in Figs. 5(e) and 5(f).

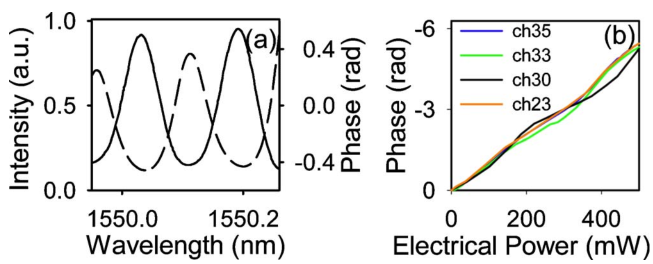

Fig. 4. (Color online) (a) Intensity transfer function (solid) and phase transfer function (dashed) of AWGPS. (b) Phase response of several resistive-heater-based phase modulators.

generated contains the phase difference between these modes.[3] This effect was used to measure the response of the phase modulators. The OFCG output passed through the AWGPS, and two modes were selected with a narrowband zero-dispersion filter. PM was applied to one of the modes. Figure 4(b) shows the phase calibration of several wavelength channels. The phase shift increases linearly with electrical power and obtains 2π phase shift at 600 mW. Using this calibration curve, the number of iterations needed to shape a given waveform is minimized. Additionally, the phase differences between each set of modes in a waveform can be measured directly to reconstruct the phase across the entire spectrum. Despite being a direct method, it has limitations, since the phase information is lost across the spectral nulls.

By using XFROG for precise mode-by-mode characterization, three interesting waveforms are generated. A pulse with quadratic spectral phase [Figs. 5(a) and 5(b)], a transform-limited pulse [Figs. 5(c) and 5(d)], and a series of pulses with increasing center frequency [Figs. 5(e) and 5(f)]. The amplitude and phases of the 32 modes were adjusted by controlling the resistive heaters in the AWGPS.

The transform-limited and quadratic spectral phase pulses are shaped to have a super-Gaussian spectrum of the form $\exp[-(f/250)^2]$, where f is the frequency axis in gigahertz in Fig. 5. The super-Gaussian shape has a flat passband and also reduces ringing in the time domain compared with a spectrum with equal-amplitude modes.

There are several difficulties in shaping pulses. Phase differences (errors) between wavelength channels within the silica AWG pair distort a pulse passing through it. The pulse input to the AWGPS [Fig. 2(b)] becomes distorted [Fig. 2(d)] after each mode obtains a different phase shift due to path-length nonuniformity in the AWGPS wavelength channels. Cross talk from inhomogeneous device heating from the resistive heaters within the OAWG change the phase and amplitude applied to the spectrum. Small amounts of cross talk (−20 dB) from phase shifts introduced by the amplitude modulator made it necessary for several iterations of measurement and correction steps to take place.

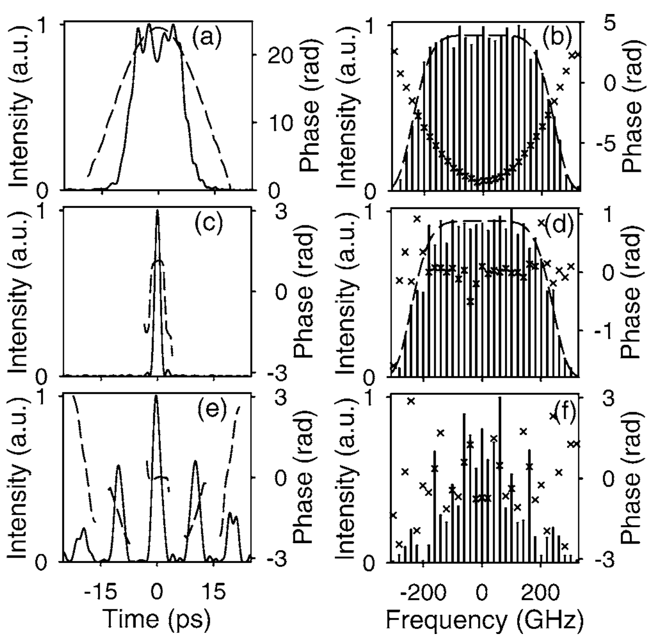

Fig. 5. Left, intensity (solid) and phase (dashed) in time domain. Right, intensity (bars) and phase (crosses) in spectral domain with target intensity (dashed). (a), (b) Linearly chirped pulse; (c), (d) flat phase pulse; (e), (f) five pulses of incremental frequency.

Figures 5(a) and 5(b) show a measured pulse with quadratic spectral phase or purely linear frequency chirp. Its pulse width is 15 ps full width at half-maximum of the intensity (FWHM). Figures 5(c) and 5(d) show a 1.5 ps FWHM pulse with flat spectral phase. Small phase errors result in noise outside the center of the pulse at 0.1%–0.5% intensity of the peak. Figures 5(e) and 5(f) show the generation of a truly complex arbitrary waveform imitating five musical notes. This waveform consists of five separate subpulses with incrementing center frequencies (different linear temporal phases). Additionally, the intensity of the waveform follows a crescendo and a decrescendo. The XFROG trace of this pulse [Fig. 3(b)] provides greater insight by showing each individual pulse's intensity, frequency, and time. The complexity of the waveform is shown in the large difference in amplitude and phase between adjacent modes in the optical spectrum. By using 32 optical modes, complex OAWG was accomplished. Further advancements in optical comb generation technology and the flexibility of FROG techniques suggest that ultracomplex OAWG will be feasible.

This work was supported in part by Defense Advanced Research Projects Agency Defense Sciences Office OAWG contract HR0011-05-C-0155. N. K. Fontaine's e-mail address is nkfontaine@ucdavis.edu.

References

1. D. Miyamoto, K. Mandai, T. Kurokawa, S. Takeda, T. Shioda, and H. Tsuda, IEEE Photon. Technol. Lett. **18**, 721 (2006).
2. A. Weiner and J. D. McKinney, in *Conference on Lasers and Electo-Optics/Quantum Electronics and Laser Science and Photonic Applications Systems Technologies*, Technical Digest (CD) (Optical Society of America, 2005), paper CTuN1.
3. Z. Jiang, D. E. Leaird, and A. M. Weiner, J. Lightwave Technol. **24**, 2487 (2006).
4. T. Sakamoto, T. Kawanishi, and M. Izutsu, in *Conference on Lasers and Electro-Optics/Quantum Electronics and Laser Science Conference and Photonic Applications Systems Technologies*, Technical Digest (CD) (Optical Society of America, 2006), paper CMAA5.
5. R. Trebino, *Frequency-Resolved Optical Gating: The Measurement of Ultrashort Laser Pulses* (Kluwer Academic, 2000).
6. N. K. Fontaine, R. P. Scott, J. Cao, K. Okamoto, J. P. Heritage, B. H. Kolner, and S. J. B. Yoo, in *European Conference on Optical Communication (ECOC)* (2006), paper We.4.6.7.
7. J. M. Dudley, F. Gutty, S. Pitois, and G. Millot, IEEE J. Quantum Electron. **37**, 587 (2001).